MULTIPLE MODEL PROPAGATION OF HIGH AREA-TO-MASS (HAMR) OBJECTS USING AN ENCKE TYPE CORRECTION ALGORITHM

Sergei Tanygin[(1)] **and James Woodburn**[(2)]
[(1)(2)]*Analytical Graphics, Inc., 220 Valley Creek Blvd., Exton, PA 19340, USA,*
[(1)]*+16109818030, stanygin@agi.com*

Abstract: *The propagation of high area-to-mass ratio (HAMR) objects is significantly affected by non-conservative attitude dependent forces. The orbit and attitude dynamics are coupled with the latter typically much faster than the former. Two important characteristics of this coupling can be taken advantage of to devise a faster propagation algorithm. First, changing attitude also affects even non-attitude dependent forces, e.g. gravitational potential and third-body forces, but only indirectly through the changes in object's position effected over time. Second, changing position and velocity affects attitude dependent torques only slightly because they arise from the difference that corresponding forces apply across the extent of an object. An Encke type correction algorithm for numerical integration that takes advantage of these characteristics was proposed in 2001. It provides a computational advantage over the fully coupled propagation by avoiding the evaluation of the dominant gravitation related forces at the high frequency demanded by the attitude dynamics. Instead, the Encke type correction is applied via a secondary integration that includes all attitude dependent effects plus the difference in the two body accelerations between the corrected and uncorrected trajectories.*

This paper examines performance of the original algorithm for a different orbit regime, and for a wider range of object shapes and attitude motions. It also introduces a modification of the algorithm for multiple model propagation (MMP). MMP involves numerical integration of multiple object models that differ in shape, mass properties and possibly initial attitude. These are used in a bank of parallel filters that eventually settle on the most probable model via a process called multiple model adaptive estimation (MMAE). The expense of running full numerical integrations of multiple competing models can be mitigated by running a full numerical integration for a single nominal model and integrating only Encke type corrections for all other models. In this approach, rectification is not applied until the MMAE algorithm settles on a single most probable model (or on a subset of most likely models).

Keywords: *orbit propagation, numerical integration, high area-to-mass ratio (HAMR) objects, multiple model propagation.*

1. Introduction

The propagation of high area-to-mass ratio (HAMR) objects is a challenging problem because of the significant effect that non-conservative attitude dependent forces exert on these objects [1]. Given that attitude dynamics may be several orders of magnitude faster than orbit dynamics, the combined effect of all forces acting on a HAMR object can be accurately captured only if all forces are evaluated at a correspondingly higher frequency. In addition to attitude dependent forces, this involves evaluation of the gravitational potential, third-body gravity contributions, gravitational effects of tides for LEO objects, etc. The influence of changing attitude on such forces is only indirect: through the changes in object's position effected over time by the attitude dependent forces. Conversely, the influence of changing position and velocity on the attitude dependent torques is typically very small due to their "differential" nature: these torques arise

from the difference that corresponding forces apply across the extent of an object. Hence, small changes in position and velocity produce only secondary effect on the torques.

The idea of splitting a complete dynamical model into several constituent parts according to their dynamical frequencies, integrating their individual contributions and assembling the results was applied to astrodynamics problems by Rowlands, D. D., et al. in 1995 [2]. In 2001, Woodburn and Tanygin [3] proposed an Encke type correction algorithm for numerical integration that appears to be particularly well suited for the HAMR propagation environment. It provides a computational advantage over the fully coupled propagation by avoiding the evaluation of the dominant gravitation related forces at the high frequency demanded by the attitude dynamics. Instead, the Encke type correction is applied via a secondary integration that includes all attitude dependent effects plus the difference in the two body accelerations between the corrected and uncorrected trajectories. The algorithm uses this integrated correction to rectify the orbit state after every main integration step which enables it to attain a better accuracy than a simple decoupled approach. For a tumbling cylinder in LEO, Woodburn and Tanygin demonstrated that their method saves up to 20% of computation time with a 12x12 degree and order truncation of the gravity potential and more with higher fidelity models, close to 75% savings with a 50x50 model. This was achieved while maintaining accuracy of better than 50 cm after 1 hour of propagation.

The Encke approach works for standard variable step size integration schemes [4, 5]. Other techniques for improving long-term accuracy and computational efficiency in challenging propagation environments have been proposed. They include symplectic and implicit integration schemes [6, 7], and integration schemes with intermittent coupling of orbit and attitude propagation determined by various entropic measures [8].

This paper examines performance of the Encke correction algorithm of Woodburn and Tanygin for a different orbit regime, and for a wider range object shapes and attitude motions compared to the original paper [3]. It also introduces a modification of the algorithm for multiple model propagation (MMP). MMP involves numerical integration of multiple object models that differ in shape, mass properties and possibly initial attitude. These are used in a bank of parallel filters that eventually settle on the most probable model via a process called multiple model adaptive estimation (MMAE) [9, 10]. The expense of running full numerical integrations of multiple competing models can be mitigated by running a full numerical integration for only one nominal model and integrating just Encke type corrections for all other models. In this case, rectification is not applied until the MMAE algorithm settles on a single most probable model (or on a subset of most likely models). Linares et al. [9] demonstrated that a correct model for objects in near GEO in a continuously-lighted trajectory can be discerned from a bank of five possible models after about 30 astrometric and photometric measurements, which amounts to about 15 min of propagation time. In a subsequent paper, Linares et al. [10] executed the MMAE algorithm on a bank of 100 models. Assuming that even without rectification integrated Encke corrections will remain sufficiently small over the MMAE interval, a bank of several models can be integrated significantly faster if all of the competing models can reuse the same reference (uncorrected) trajectory. For example, based on the original results of Woodburn and Tanygin [3], integrating five object models with a 12x12 gravity potential model can be expected to save significantly more than 20% of computation time, with the savings being proportional to the number of models. This makes the Encke correction approach uniquely suitable to improve the shape and attitude estimation of the HAMR objects by evaluating a greater number of competing models within the same computational constraints.

2. Formulation

The original Encke correction approach advocated by Woodburn and Tanygin [3] involves the main orbit integrator which accounts for all non-attitude dependent forces and the corrector integrator which accounts for all attitude dependent forces and the differential two-body contribution and if necessary integrates the attitude motion. After the main orbit integrator takes a single step, the corrector integrator propagates both orbit corrections and attitude over that step. In this process, it requires the uncorrected orbit state, which it obtains via interpolation of the uncorrected ephemeris, to assemble the fully corrected state for its attitude dependent force models. The uncorrected ephemeris is rectified and the main orbit integrator uses the fully corrected state to start another step (Fig. 1).
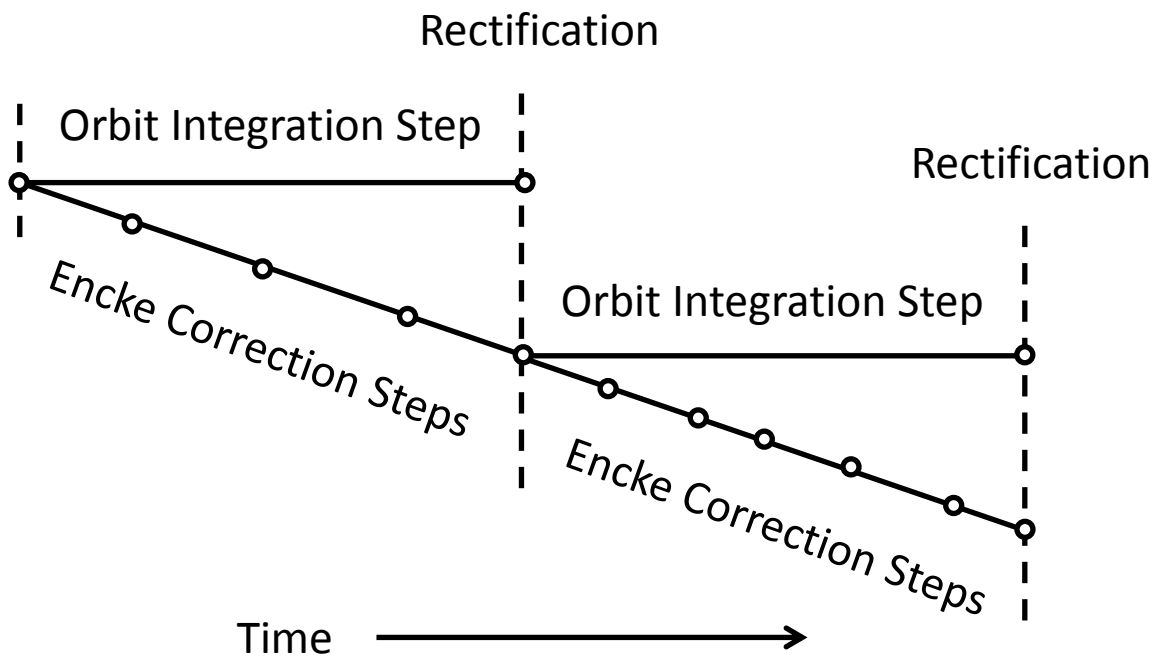
Figure 1: Encke correction approach

In this paper, the Encke correction approach is modified and applied to the MMAE process which involves running a bank of parallel filters each using its own candidate dynamical model. The MMAE process culminates when it identifies the most likely model. The Encke approach in this paper is modified in two ways: it foregoes rectifications after main orbit integration steps and executes sequences of Encke correction steps for each candidate model with corrections in each case applied with respect to the same nominal uncorrected orbit (Fig. 2).
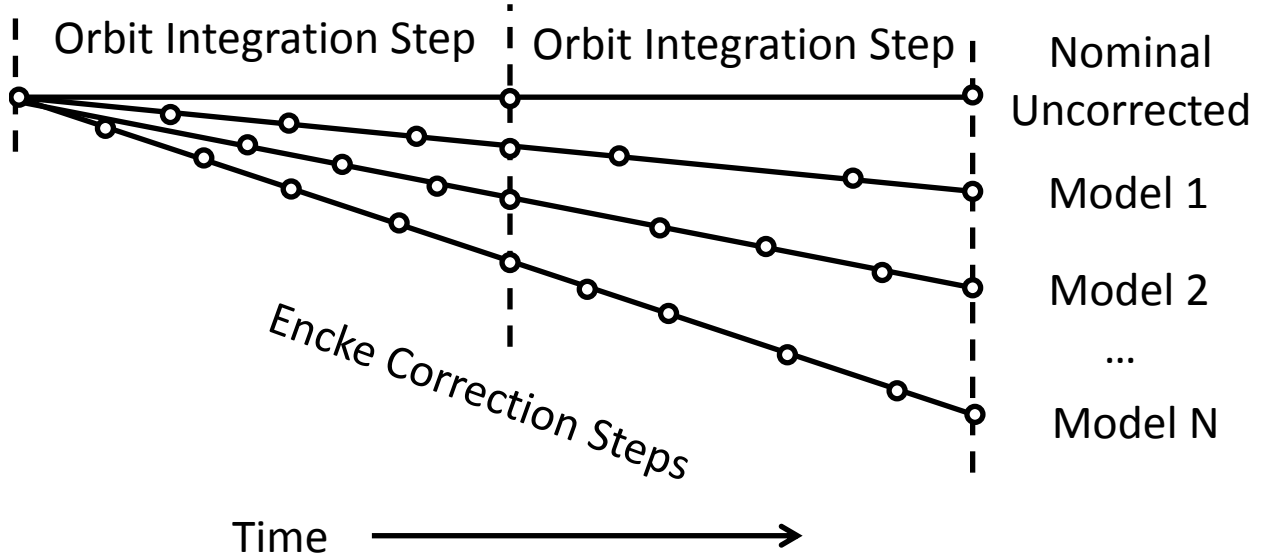
Figure 2: MMP using Encke corrections for MMAE

As with the original Encke approach, computational savings are realized because costly evaluations of the gravity potential (and of other forces not explicitly dependent on attitude) are carried out only during main orbit integration steps and, consequently, are evaluated less frequently than the fully-coupled integration would have required. The MMP Encke approach further multiplies these savings by foregoing rectifications and using the same uncorrected ephemeris as a reference for integrated corrections of all dynamical models adopted within MMP. Of course, this assumes that the MMAE process can successfully identify the most likely model before the corrections become so large that the accumulated differential effects of higher order gravitational potential invalidate the analysis.

Following Woodburn and Tanygin [3], the equations of motion for the main orbit integrator can be presented either in the attitude or in the extended correction formulations. The former includes some averaged a priori determined contributions from the attitude dependent forces while the latter does not. Given the variety and complexity of models that may be considered in the MMAE process, it may be difficult to determine appropriate averaged contributions. Hence, only the extended correction formulation is considered in this work. In this formulation, the reference uncorrected trajectory is governed by the following equations of motion

$$\ddot{\boldsymbol{\rho}} = \nabla U + \mathbf{a}_{Sun} + \mathbf{a}_{Moon} . \tag{1}$$

Here ∇U is the gradient of the gravitational potential function, $\mathbf{a}_{Sun}$ and $\mathbf{a}_{Moon}$ are the third body gravitational accelerations due to the Sun and the Moon, respectively.

The orbit corrections are realized through the integration of attitude dependent contributions of drag and SRP accelerations (due to attitude dependent areas). The corrections are governed by

$$\Delta \ddot{\mathbf{r}} = \frac{\mu}{\|\boldsymbol{\rho}\|^3} \left[\left(1 - \frac{\|\boldsymbol{\rho}\|^3}{\|\mathbf{r}\|^3} \right) \mathbf{r} - \Delta \mathbf{r} \right] + \mathbf{a}_{drag} + \mathbf{a}_{SRP} , \tag{2}$$

4

where μ is the gravitational parameter, $\mathbf{r}$ and $\mathbf{\rho}$ denote the corrected and uncorrected states, respectively, which are related simply via $\mathbf{r} = \mathbf{\rho} + \Delta\mathbf{r}$.

The original approach calls for rectifications after each main orbit integration step (see Fig. 1) but, in the context of MMP, the tabulated uncorrected ephemeris, $\mathbf{\rho}(t)$ for $t \in \left[t_0, t_f\right]$, is produced only once and without rectifications over the entire period of interest, and the corrections, $\Delta\mathbf{r}_k(t)$ for $t \in \left[t_0, t_f\right]$ are produced for each candidate dynamical model, $k = 1, 2, ..., N$. The uncorrected states are recorded at the main orbit integrator steps and are made available at various intermediate times via interpolation of tabulated values (see Fig. 2).

This paper focuses on orbit regimes where the drag acceleration is insignificant. The general formulation of the SRP acceleration adopted in this paper is for a convex body with L facets. The formulation is expressed as a sum of SRP accelerations from individual facets:

$$\mathbf{a}_{SRP} = -\kappa \frac{F_{mean}}{Mcd^2} \sum_{l=1}^{L} A_{(l)} \lambda_{(l)}^2 \mathbf{u}_{SRP(l)} , \tag{3a}$$

where $\kappa \in [0,1]$ is the fraction of visible solar disk, M is the total mass of the object, F_{mean} is the mean solar flux at 1 AU, c is the speed of light, d is the distance to the apparent Sun measured in AU. The terms for the l-th facet include the total area, $A_{(l)}$, as well as

$$\lambda_{(l)} = \max[0, \hat{\mathbf{s}}^T \hat{\mathbf{n}}_{(l)}] , \tag{3b}$$

and

$$\mathbf{u}_{SRP(l)} = 2\left[\frac{R_{diff(l)}}{3} + \frac{R_{abs(l)}\varepsilon_{(l)}}{3} + R_{spec(l)}\lambda_{(l)}\right]\hat{\mathbf{n}}_{(l)} + \left[1 - R_{spec(l)}\right]\hat{\mathbf{s}} , \tag{3c}$$

where $\hat{\mathbf{s}}$ is the unit vector to the apparent Sun and where, for the l-th facet, $\varepsilon_{(l)}$, $R_{diff(l)}$, $R_{abs(l)}$, and $R_{spec(l)}$ are the emissivity, diffuse reflectance, absorption and specular reflectance coefficients, respectively, and $\hat{\mathbf{n}}_{(l)}$ is the unit (outward) surface normal.

The equations of motion for the attitude state, assuming rigid body motion, are

$$\dot{\mathbf{q}} = \frac{1}{2}\mathbf{\Omega}(\mathbf{\omega}^B)\mathbf{q} , \tag{4a}$$

$$\dot{\mathbf{\omega}}^B = \mathbf{J}^{-1}\left(\mathbf{T}^B - \mathbf{\omega}^B \times \mathbf{J}\mathbf{\omega}^B\right) , \tag{4b}$$

where $\mathbf{q}$ is the 4x1 unit quaternion column-vector representing the object's body frame with respect to some known inertial reference frame, e.g. ICRF, $\mathbf{\omega}^B$ is the angular velocity vector of the object with respect to that inertial reference expressed in the object's body frame, $\mathbf{J}$ is the object's inertia matrix, $\mathbf{T}$ is the total external torque acting on the object expressed in its body

5

frame, and $\mathbf{\Omega}(\boldsymbol{\omega})$ is the 4x4 skew-symmetric matrix defined as

$$\mathbf{\Omega}(\boldsymbol{\omega}) = \begin{bmatrix} -[\boldsymbol{\omega}\times] & \boldsymbol{\omega} \\ -\boldsymbol{\omega}^T & 0 \end{bmatrix}. \tag{4c}$$

Similar to the SRP acceleration, the torque due to SRP is given as a sum of torque contributions from individual facets:

$$\mathbf{T}_{SRP}^{B} = M \sum_{l=1}^{L} \boldsymbol{\rho}_{(l)}^{B} \times \mathbf{a}_{SRP(l)}^{B} . \tag{5}$$

In the derivations above, all Cartesian vector quantities are expressed in the inertial frame except those tagged with superscript B which are expressed in the object's body frame. Transformations of vector quantities between inertial and body frames are carried out using a direction cosine matrix constructed from the inertial-to-body quaternion $\mathbf{q}$.

3. Test cases

The approach is evaluated using a rectangular cuboid shape model which is defined by the two orthogonal base sides, s_1 and s_2, and the height, h (see Fig. 3).
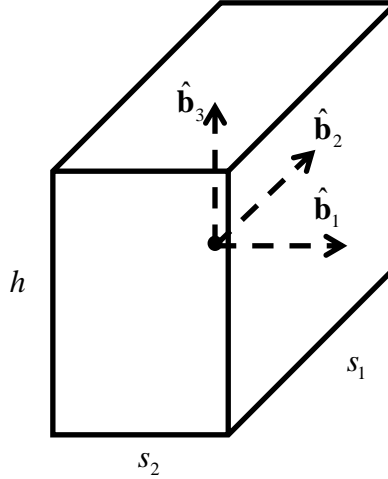
Figure 3: Rectangular cuboid shape model for SRP

The inertia matrix for this shape is given by

$$\mathbf{J} = \frac{M}{12} \begin{bmatrix} s_2^2 + h^2 & 0 & 0 \\ 0 & s_1^2 + h^2 & 0 \\ 0 & 0 & s_1^2 + s_2^2 \end{bmatrix}. \tag{6}$$

The total areas, unit (outward) normal vectors and centroid locations of each facet in the body fixed frame are given in Table 1:

6

Table 1. Areas, Normals and Centroid Locations of Each Facet

i	$A_{(i)}$	$\left[\hat{\mathbf{n}}^B_{(i)}\right]^T$	$\left[\boldsymbol{\rho}^B_{(i)}\right]^T$
1	$s_1 s_2$	$\begin{bmatrix} 0 & 0 & -1 \end{bmatrix}$	$\begin{bmatrix} 0 & 0 & -h/2 \end{bmatrix}$
2	$s_2 h$	$\begin{bmatrix} 0 & -1 & 0 \end{bmatrix}$	$\begin{bmatrix} 0 & -s_1/2 & 0 \end{bmatrix}$
3	$s_1 h$	$\begin{bmatrix} 1 & 0 & 0 \end{bmatrix}$	$\begin{bmatrix} s_2/2 & 0 & 0 \end{bmatrix}$
4	$s_2 h$	$\begin{bmatrix} 0 & 1 & 0 \end{bmatrix}$	$\begin{bmatrix} 0 & s_1/2 & 0 \end{bmatrix}$
5	$s_1 h$	$\begin{bmatrix} -1 & 0 & 0 \end{bmatrix}$	$\begin{bmatrix} -s_2/2 & 0 & 0 \end{bmatrix}$
6	$s_1 s_2$	$\begin{bmatrix} 0 & 0 & 1 \end{bmatrix}$	$\begin{bmatrix} 0 & 0 & h/2 \end{bmatrix}$

In order to validate selected dynamical models and highlight the advantages of the Encke correction approach, it is instructive to choose an orbit that experiences notable contributions from higher gravity field harmonics, third-body effects and SRP, but not from atmospheric drag. In order to realize the benefits of this approach, it is also instructive to consider bodies experiencing rotational motions that are fast enough to undergo many revolutions within the time span of MMAE process. To this end, a MEO is selected with the orbital period of about 4 hours. Three tests are performed using different initial angular velocities of the object's body: one with the object's rotational period of about 2 min, the second with the period of about 20 min and the final test with a rotational period of about 200 min. This means that during the first test, the rotational dynamics are about 120 times faster than orbital dynamics, during the second test they are about 12 times faster and during the final test the rotational dynamics are at nearly the same rate as the orbital dynamics. The orbit and attitude parameters are listed in Table 2.

The object mass is 1000 kg. The dynamical models include 20x20 WGS84 EGM96 gravity field, the Sun and Moon third body point mass effects, and the effect of SRP on both translational and rotational motions. The tests are performed using a single cuboid model described in Table 3 and also using a bank of 100 randomly generated cuboid models with dimensions uniformly distributed between 1 and 5 m. The numerical integrator in all tests is the variable step Runge–Kutta–Fehlberg 7(8)th order integrator [11] with relative error control threshold set to 10^{-13}. Parameters of the cuboid shape model that is used to demonstrate accuracy results are listed in Table 3.

Table 2. Orbit and Attitude Parameters

Parameters	Values	
Epoch, t_0	15 Apr 2014 16:00:00 UTCG	
Initial Position, $\mathbf{r}_0$ (km)	$\begin{bmatrix} 3483.21882071397 \\ -6550.75966751559 \\ 9499.27574186805 \end{bmatrix}$	
Initial Velocity, $\mathbf{v}_0$ (km/s)	$\begin{bmatrix} 5.39961448365528 \\ 1.97873529145312 \\ -0.534275901579994 \end{bmatrix}$	
Initial Attitude, $\mathbf{q}_0^T$	$\begin{bmatrix} 1.0 & 0.0 & 0.0 & 0.0 \end{bmatrix}$	
Initial Angular Velocity, $\boldsymbol{\omega}_0^T$ (deg/s)	Fast Test	$\begin{bmatrix} 3.0 & 2.0 & 1.0 \end{bmatrix}$
	Medium Test	$\begin{bmatrix} 0.3 & 0.2 & 0.1 \end{bmatrix}$
	Slow Test	$\begin{bmatrix} 0.03 & 0.02 & 0.01 \end{bmatrix}$

Table 3. Cuboid Shape Model Parameters

Parameters	Values
$\{s_1, s_2, h\}$ (m)	$\{2.0, 1.0, 4.0\}$
$\{\varepsilon_{(l)}, R_{spec(l)}, R_{diff(l)}, R_{abs(l)}\}$, $l = 1,...,6$	$\{0.5, 0.7, 0.3, 0.0\}$

4. Accuracy results

The Encke approaches are tested for both long-term and short-term accuracy, and computational efficiency. It is instructive to examine the dynamical environment for the selected MEO. The contributions of various effects to the overall inertial acceleration are plotted in Fig. 4.

Fast test. Accuracy of the fast test with initial angular rates of up to 3 deg/s is examined in Figs. 5 and 6. Figure 5 includes comparisons of position differences between orbits propagated using

8

different techniques and the "true" orbit generated by the fully coupled propagation of orbit and attitude states. The orbit propagated without SRP is the reference orbit used for the Encke methods. Propagated over a day, it differs from the fully coupled orbit by up to 30 m. The orbit propagated using average SRP uses a spherical shape model with the cross-section of 20 m^2 and the coefficient of reflectivity of 2.2. Over a day, it differs from the fully coupled orbit by up to 10 m. The orbits propagated using Encke corrections remain much closer to the fully coupled orbit: within about 1 cm for the unrectified Encke method and within about 0.5 mm for the original Encke method. Within the first hour, the corresponding orbit errors are about 1 m without any SRP, about 10 cm with average SRP, about 0.1 mm with unrectified Encke corrections and close to 0.05 mm with rectified Encke corrections.
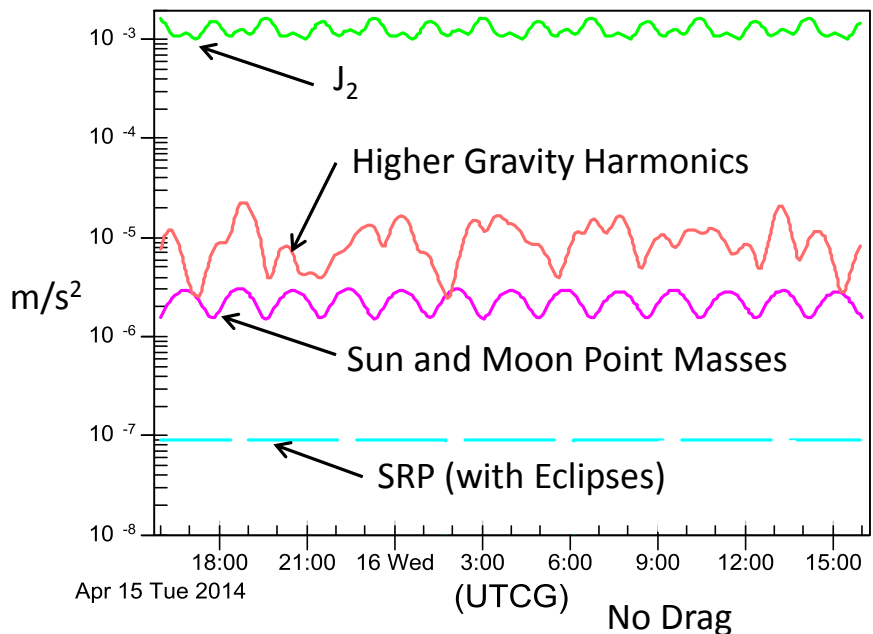
Figure 4: Contributions of Various Accelerations along Selected MEO
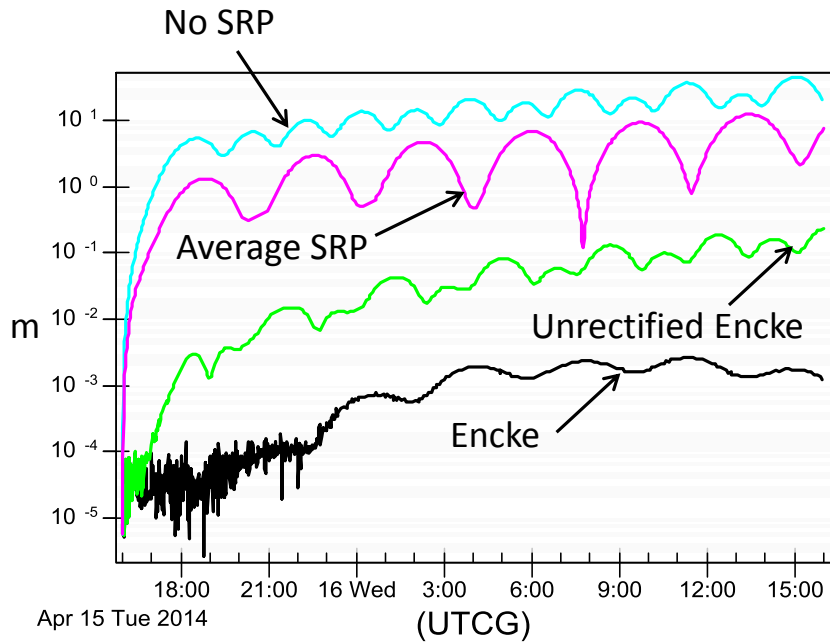
9
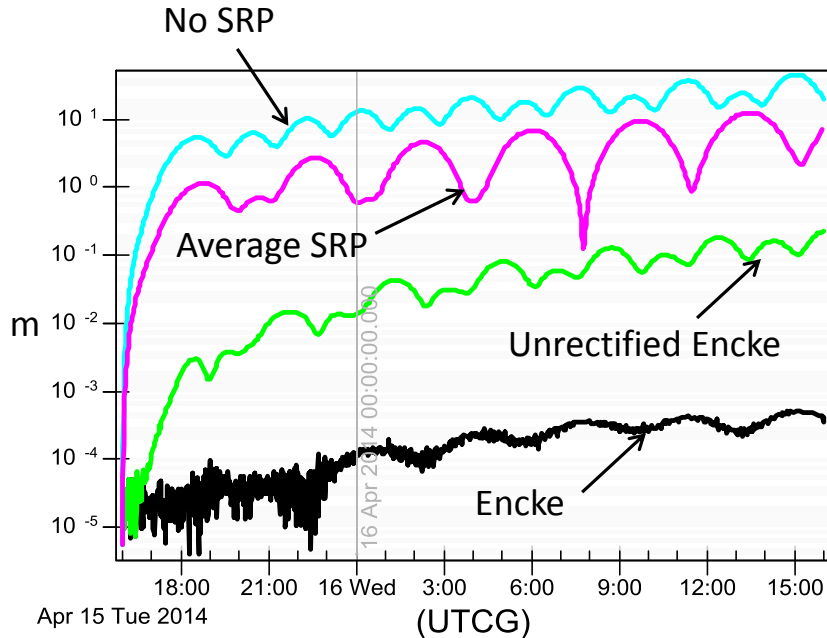
Figure 5: Position Differences between Various Propagation Methods and Fully Coupled Propagation during Fast Test

Figure 6 includes comparisons of rotation angle differences between different attitude propagation techniques and the "true" attitude which is once again represented by the fully coupled propagation of orbit and attitude states. The techniques include the attitude states propagated decoupled from orbit states without considering SRP torque, which is what happens for models either without SRP or with spherical average SRP, and the attitude states propagated using Encke corrections. Over a day, the decoupled attitude propagation results in errors of up to 1.8 deg, while the partially coupled Encke corrected propagation (with or without orbit rectifications) results in errors of up to 0.5 deg.
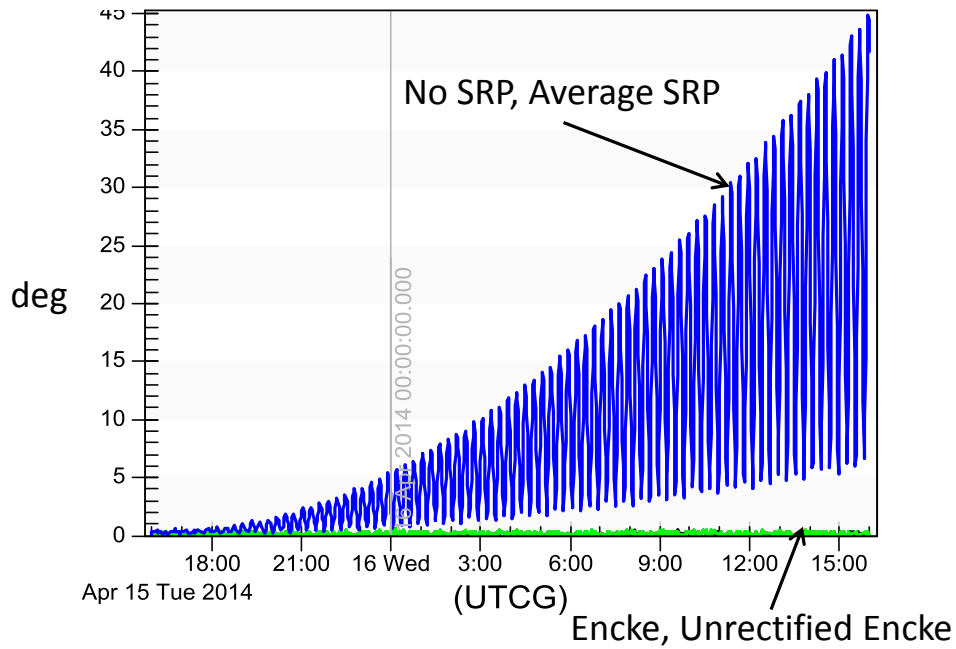
Medium test. For the medium test, the initial angular rates are reduced by a factor or 10. The corresponding position and attitude accuracy results are shown in Figs. 7 and 8. The position results for the medium test are quite similar to those for the fast test (compare Figs. 7 and 5). However, the attitude results are markedly different (compare Figs. 8 and 6). The uncoupled attitude propagation suffers from much larger errors that grow up to 45 deg, while the partially coupled Encke corrected propagation maintains its errors below 0.5 deg. A dramatic loss of attitude accuracy during the medium test compared to the fast one is likely due to the fact that the small asymmetries of SRP forces acting across the shape, which generate the SRP torque, are able to persist longer and affect attitude more during relatively slow rotations. During the fast test, the rotation rate remains so high that the asymmetries that exist at one time are getting cancelled out almost immediately by subsequent opposite asymmetries resulting in comparatively negligible effect on the propagated attitude. Hence, the net effect on the attitude is much closer to torque-free.
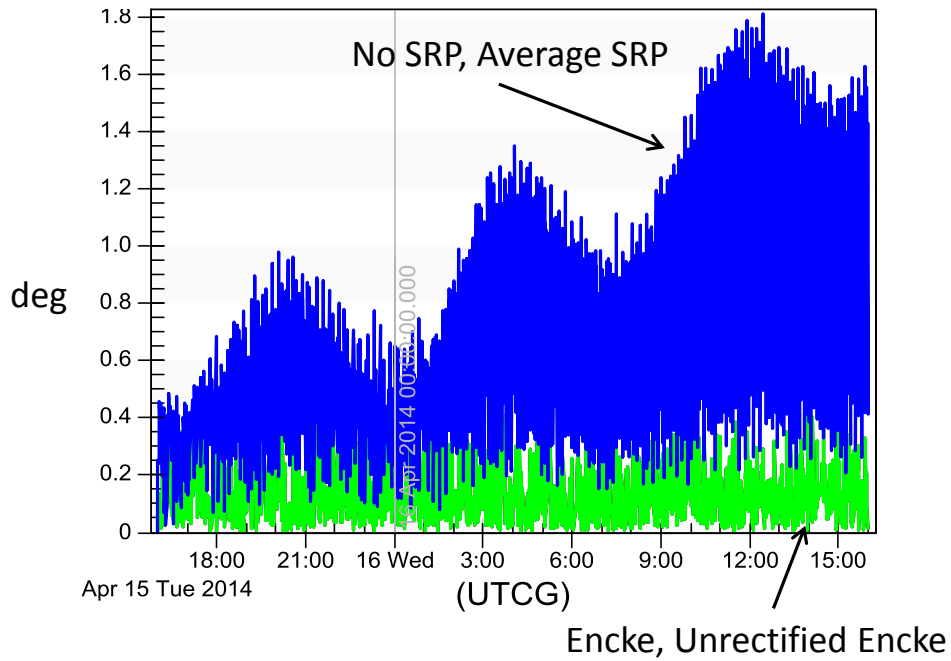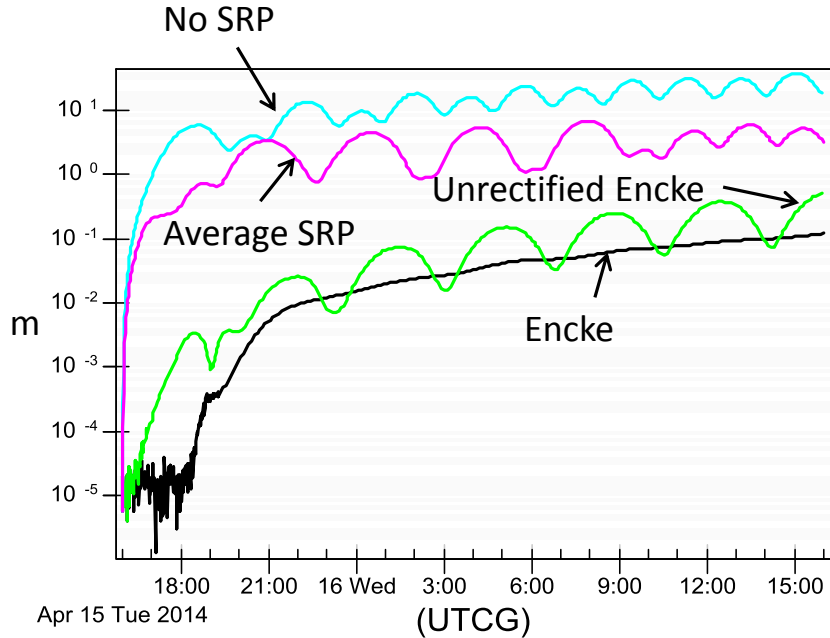
Figure 6: Rotation Differences between Various Propagation Methods and Fully Coupled Propagation during Fast Test
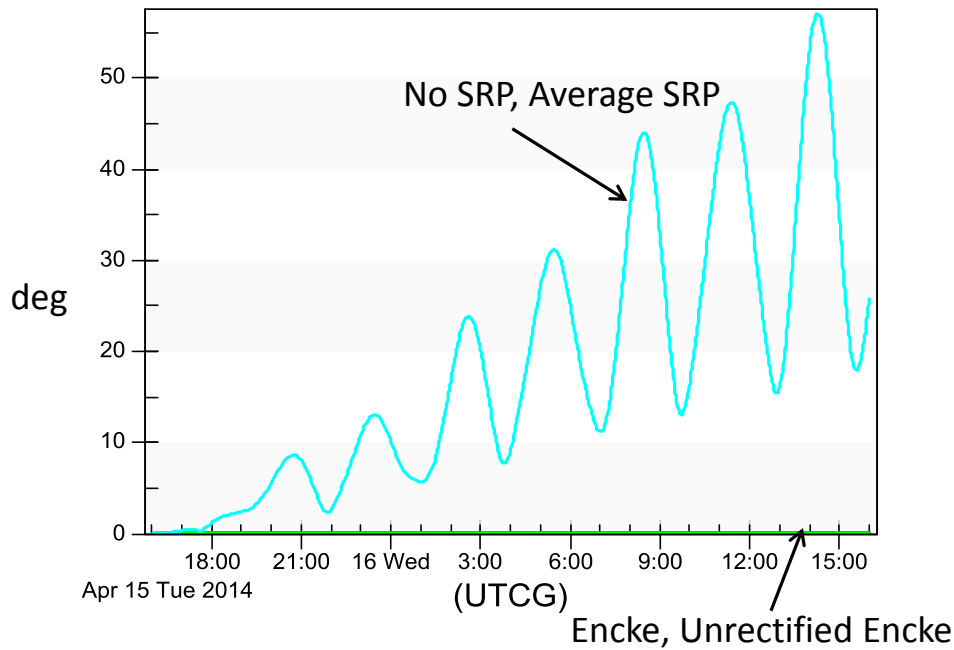

Figure 7: Position Differences between Various Propagation Methods and Fully Coupled Propagation during Medium Test

11

Figure 8: Rotation Differences between Various Propagation Methods and Fully Coupled Propagation during Medium Test

Figure 9: Position Differences between Various Propagation Methods and Fully Coupled Propagation during Slow Test

Figure 10: Rotation Differences between Various Propagation Methods and Fully Coupled Propagation during Slow Test

Slow test. For the slow test, the initial angular rates are reduced further by a factor or 10. The corresponding position and attitude accuracy results are shown in Figs. 9 and 10. The Encke corrected position errors for the slow test are somewhat larger than those for the fast and medium tests (compare Fig. 9 to Figs. 5 and 7). This likely is a byproduct of longer step sizes taken during Encke corrections which, in turn, are due to slower attitude dynamics. Still, the Encke corrected position errors and, especially, attitude errors are markedly better than those without corrections (Figs. 9 and 10). The uncoupled attitude propagation produces even larger errors (up to about 55 deg) during the slow test than during the medium test (compare Figs 10 and 8). The partially coupled Encke corrected propagation actually improves during the slow test maintaining errors below 0.05 deg compared to 0.5 deg during the medium test.

Having established the accuracy of Encke approaches, it is now important to examine whether they are computationally efficient.

5. Computational efficiency results

In order to explain how computational gains are realized by the Encke approaches, it is instructive to examine the number of samples taken by the variable step integrator.
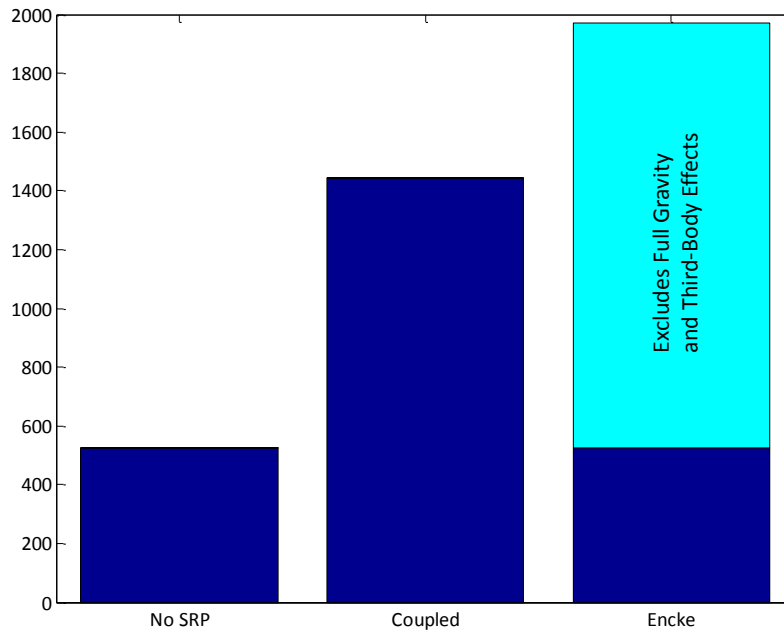
Fast test. The numbers of orbit samples taken over a day during the fast test are shown in Fig. 11. It demonstrates how the inclusion of the fast attitude dynamics dramatically increases the number of orbit samples needed by the variable step integrator between the uncoupled propagation without SRP and the fully coupled propagation. Overall, the Encke approach requires even more samples but it combines evaluations of two significantly different force

13

models. The bottom of its bar chart depicts evaluations of the full gravity and third-body effects, which are equal in number to similar evaluations performed during the uncoupled propagation. The top of its bar chart depicts evaluations of Encke correction force and torque models which exclude the full gravity and third-body effects and use interpolation to access the reference orbit propagated during the main orbit steps. Hence, the efficiency of the Encke approaches hinges on making these Encke correction evaluations much faster than their fully coupled counterparts.

Medium test. The numbers of orbit samples taken over a day during the medium test are shown in Fig. 12. As expected, the number of orbit samples taken during uncoupled propagation without SRP remains the same, but the number of orbit samples taken during the coupled propagation is reduced by about a factor of 10 which correlates with the corresponding reduction of the attitude rates. Note that, proportionally, the number of uncoupled "no SRP" evaluations is now greater compared to the number of fully coupled evaluations. This means that the effectiveness of Encke approaches is now also reduced as evident in Fig. 12.
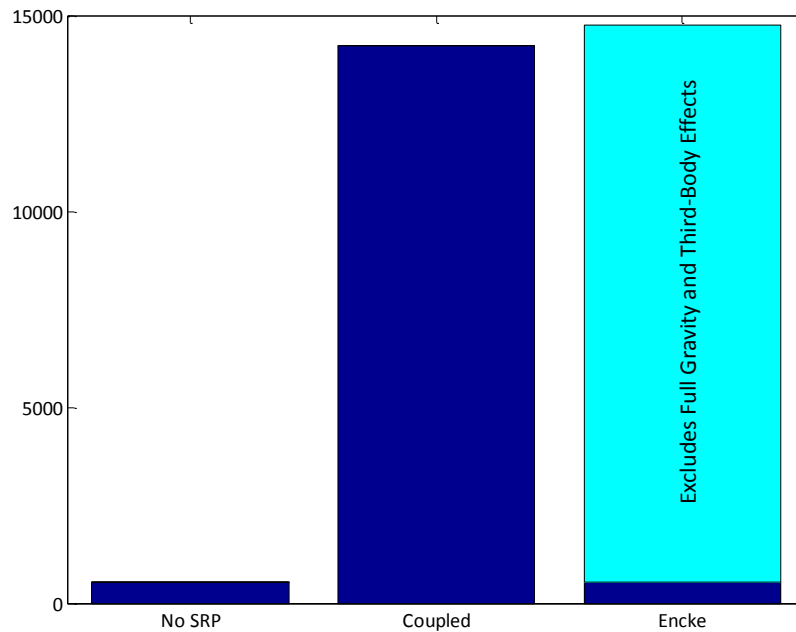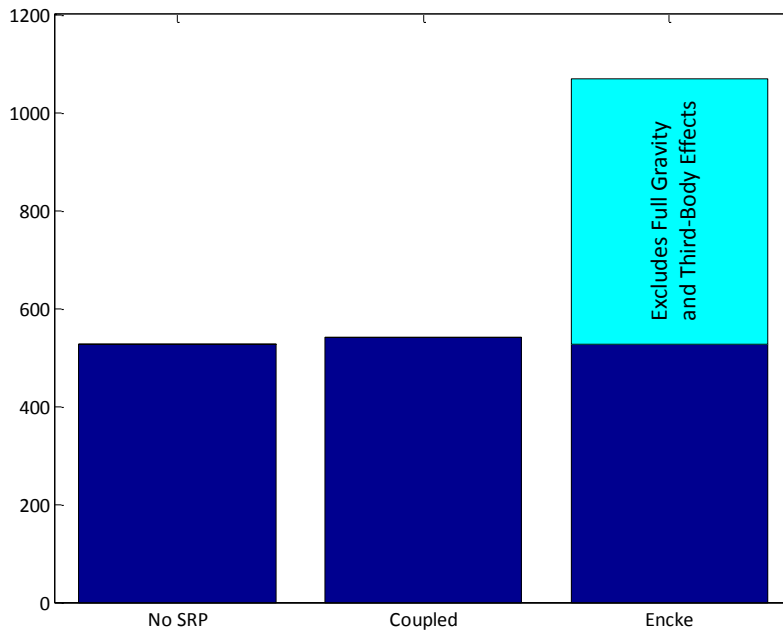

Figure 11: Numbers of Orbit Samples taken during Fast Test

Figure 12: Numbers of Orbit Samples taken during Medium Test

Slow test. The slow test demonstrates this effect even more clearly. This time the number of orbit samples taken during the coupled propagation is reduced further by a factor of 3. This makes the number coupled evaluations only slightly greater than the number of uncoupled ones, which means that the overall number of evaluations during the Encke approaches is now about twice as big as the number of coupled evaluations (Fig. 13). Hence, the effectiveness of these approaches is now significantly reduced.

Comparing the number of evaluations demonstrates internal mechanizations of different methods but by itself does not provide direct evidence of computational efficiency. This is because the Encke approaches include two different types of force/torque model evaluations: the main orbit integrator evaluates full gravity and third-body effects and the correction integrator evaluates differential two-body and attitude-dependent effects. Computational efficiency can be examined directly by comparing relative execution times of different methods. Instead of comparing these times for a propagation of a single shape model, which would produce essentially identical results for both the original and the unrectified Encke methods, the comparison is carried out after an execution of 100 propagations, one for each of the randomly generated rectangular cuboid shape models. This does not alter relative relationships between execution times of the uncoupled "no-SRP" and fully coupled propagations, and the propagations using the original Encke method. But it does give a computational advantage to the unrectified Encke method because in this case the method would only evaluate the reference orbit once and would reuse this orbit for all 100 correction propagations.

Figure 13: Numbers of Orbit Samples taken during Slow Test

Fast test. As expected, the fast test proves to be the most efficient for the Encke approach. The fully coupled propagation is about 34 times slower than the uncoupled propagation without SRP. On the other hand, the Encke and the unrectified Encke methods are less than 20 times slower than the uncoupled propagation (Fig. 14). Hence, these methods produce noticeably better accuracy then the uncoupled propagation (Figs. 5 and 6) at what turns out to be a fraction of the computational cost. Note that the unrectified Encke method is only marginally more efficient than the original Encke method. Somewhat counterintuitively, this happens because the cost of the reference orbit propagation is quite small compared to the cost of the fully coupled propagation. In other words, the original Encke method is already very efficient in this case and the computational gains achieved by reusing the same reference orbit by the unrectified Encke method are comparatively insignificant.

Medium test. The medium test demonstrates that the Encke method propagation, while still faster than the fully coupled propagation, becomes significantly less efficient (Fig. 15). The drop in the efficiency of the Encke method is due to the fact that the fully coupled propagation is now only about 3.4 times slower than the uncoupled propagation without SRP, which correlates with the corresponding change in the number of evaluations (compare Figs. 11 and 12 with Figs. 14 and 15). At the same time, this provides an opportunity for the unrectified Encke method to gain a more substantial relative advantage by reusing the same reference orbit for all 100 correction propagations. The unrectified Encke propagation is only about 2 times slower than the uncoupled propagation without SRP compared to the original Encke propagation which is about 3 times slower. Recall that in this test, the accuracy of the attitude propagation in particular is orders of magnitude better for the Encke approaches than for the uncoupled approach (Figs. 7 and 8).
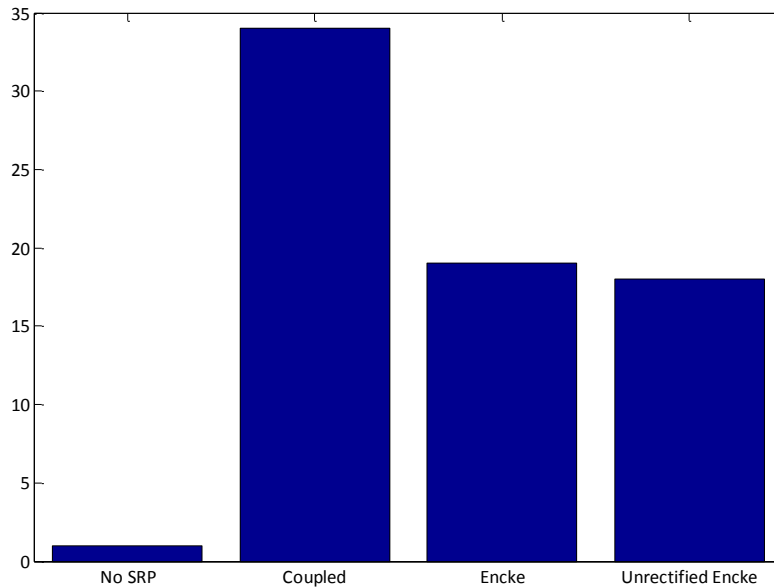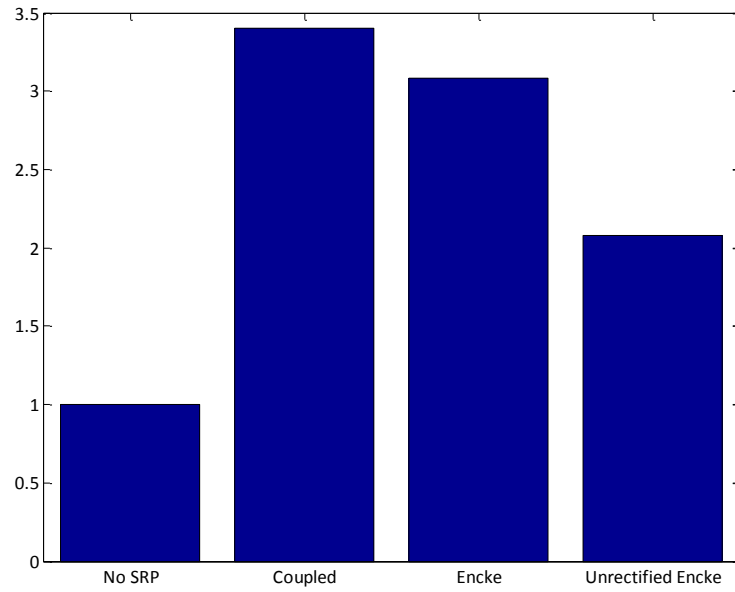
Figure 14: Relative Execution Times for 100 Models during Fast Test

Slow test. The slow test demonstrates the ultimate advantage of the unrectified Encke method for the propagation of multiple models. In this test, the fully coupled propagation is only about 20% slower than the uncoupled propagation without SRP. This makes the original Encke method even more inefficient: its propagation is about 60% slower than the uncoupled propagation, so it is actually slower than the fully coupled propagation. However, because the uncoupled propagation of the reference orbit now takes such a significant portion of the fully coupled propagation, reusing the same reference orbit for all 100 correction propagations makes a substantial impact on the overall execution time. The net result is that, for 100 models, the unrectified Encke propagation is now about twice as fast as the fully coupled propagation. Furthermore, it is even faster than 100 uncoupled propagations (Fig. 16)! And, of course, the unrectified Encke propagation is still significantly more accurate than the uncoupled propagation (Figs. 9 and 10).

It should be noted that the efficiency of access to the reference orbit during Encke correction steps is paramount for the overall efficiency of the Encke methods. The optimized implementation of these methods includes storing the current and previous states of the reference orbit for quick access during interpolation and using fast two point variation of parameter (VOP) interpolation.

6. Conclusions

The efficacy of the original Encke approach, which applies differential two-body and attitude dependent corrections to the numerically integrated reference orbit, has been demonstrated for a rectangular cuboid object in MEO subjected to attitude dependent SRP effects. A modification of the original approach that foregoes reference orbit rectifications and reuses the same reference orbit to propagate corrections for multiple models has been introduced. It has been shown that this unrectified Encke approach can yield substantial computational gains for the multiple model propagation (MMP), which is part of the multiple model adaptive estimation (MMAE) process.

Figure 15: Relative Execution Times for 100 Models during Medium Test
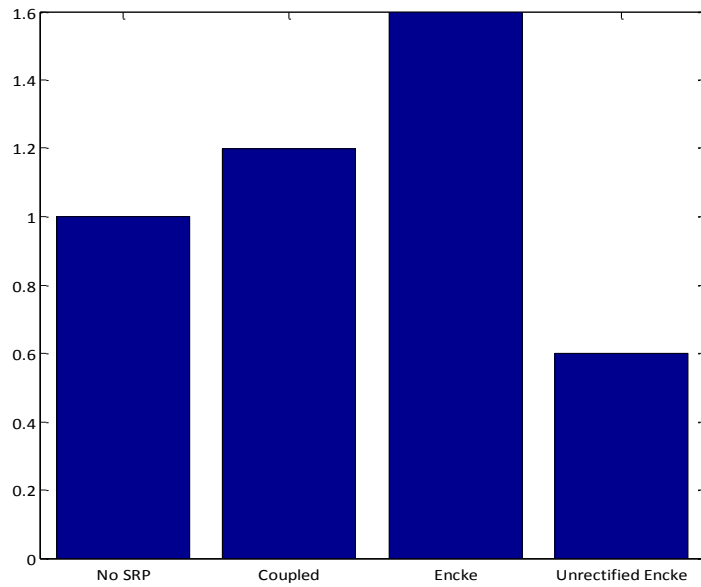
Figure 16: Relative Execution Times for 100 Models during Slow Test

7. Acknowledgements

8. References

[1] Früh, C., Kelecy, T. M., and Jah, M. K., "Coupled orbit-attitude dynamics of high area-to-mass ratio (HAMR) objects: influence of solar radiation pressure, Earth's shadow and the visibility in light curves," *Celestial Mechanics and Dynamical Astronomy*, December 2013, Volume 117, Issue 4, pp 385-404.

[2] Rowlands, D. D., et al., "Multi-Rate Numerical Integration of Satellite Orbits for Increased Computational Efficiency," *The Journal of the Astronautical Sciences*, Vol. 43, No. 1, 1995, pp. 89-100.

[3] Woodburn, J. and Tanygin, S., "Efficient Numerical Integration of Coupled Orbit and Attitude Trajectories Using an Encke Type Correction Algorithm," Paper AAS 01-428, AAS/AIAA Astrodynamics Specialist Conference, Quebec City, Quebec, Canada, July 30-August 2, 2001.

[4] Montenbruck, O. and Gill, E., *Satellite Orbits: Models, Methods, and Applications*, Springer, Berlin, 2000.

[5] Vallado, D. A., *Fundamentals of Astrodynamics and Applications*, 2nd ed., Microcosm Press, El Segundo, CA and Kluver Academic Publishers, Dordrecht, The Netherlands, 2001.

[6] Jones, B. A. and Anderson, R. L., "A survey of symplectic and collocation integration methods for orbit propagation," Proceedings of the 22nd Annual AAS/AIAA Space Flight Mechanics Meeting, AAS 12-214, Charleston, SC, Jan. 30 - Feb. 2, 2012, pp. 1-20.

[7] Aristoff, J. M. and Poore, A. B., "Implicit Runge-Kutta methods for orbit propagation," in Proceedings of the 2012 AIAA/AAS Astrodynamics Specialist Conference, AIAA 2012-4880, Minneapolis, MN, August, 2012, pp. 1-19.

[8] Früh, C. and Jah, M. K., "Attitude and Orbit Propagation of High Area-to-Mass Ratio (HAMR) Objects Using a Semi-Coupled Approach," Proceedings of AAS/AIAA Spaceflight Mechanics Meeting, AAS 13-485, Kauai, HI, 2013, Advances in the Astronautical Sciences, Vol. 148, 2013.

[9] Linares, R., Crassidis, J. L., Jah, M. K., and Kim, H., "Astrometric and Photometric Data Fusion for Resident Space Object Orbit, Attitude and Shape Determination Via Multiple-Model Adaptive Estimation," Paper AIAA 2010-8341, AIAA Guidance, Navigation and Control Conference, Toronto, Ontario, Canada, August 2 - 5, 2010.

[10] Linares, R., Jah, M. K., Crassidis, J. L., and Nebelecky, C. K., "Space Object Shape Characterization and Tracking Using Light Curve and Angles Data," Journal of Guidance, Control, and Dynamics, Vol. 37, No. 1, January - February, 2014, pp. 13-25.

[11] Fehlberg, E., "Some Old and New Runge-Kutta Formulas with Stepsize Control and Their Error Coefficients," *Computing*, Vol. 34, 1985, pp. 265-270.